Modeling dynamics and thermodynamics of icebergs in the Barents sea: 1987-2005

I. Keghouche, F. Counillon, L. Bertino (Contact: intissar.keghouche@nersc.no)

A model study on icebergs drift characteristics in the Barents and the Kara Sea for the period 1987-2005 is presented. Maps of icebergs density and potential locations subject to grounding complement sparse existing oceanographic and aerial field campaigns. The model reproduces typical pathways given by the observations and suggests a more complete picture. Icebergs originating from Franz Josef Land have the largest spread over the domain though it is not the main iceberg production site. We observe a strong interannual variability of the iceberg extent with a weak decreasing trend, similarly to the observed sea ice extent. Analysis of the atmospheric forcing reveals that years with anomalous northerly winds enhance iceberg extension. Northerly winds have also a delayed positive impact on the iceberg extent. They limit the inflow of Atlantic Water into the Barents Sea and therefore its heat content the following year, increasing the mean age of iceberg and thus their potential extension. Finally, the model is able to reproduce the observed extreme iceberg extension south east of the Barents Sea in May 2003.

MODEL

The iceberg drift model

The basic equation describing the horizontal motion of an iceberg of mass M is:

$$M\frac{d\vec{u}}{dt} = \vec{F}_{\rm A} + \vec{F}_{\rm W} + \vec{F}_{\rm C} + \vec{F}_{\rm SS} + \vec{F}_{\rm SI}, \quad (1)$$

where $\vec{u}$ is the iceberg velocity. The atmospheric force ($\vec{F}_{\rm A}$) and ocean force ($\vec{F}_{\rm W}$) act on the cross-sectional area above (resp. below) the water line in a vertical plane (form drag) and a horizontal plane (surface drag).$\vec{F}_{\rm C}$ is the Coriolis force, $\vec{F}_{\rm SS}$ is the force due to the sea surface slope and $\vec{F}_{\rm SI}$ is the force due to interaction with the sea ice cover. Note that $\vec{F}_{\rm SI}$ depends nonlinearly on the sea ice concentration A and the sea ice strength P (*Lichey and Hellmer, 2001*):

$$\mathbf{F}_{\rm SI} = \begin{cases} 0 & \text{if } A \le 15\%, \\ -(\mathbf{F}_{\rm A} + \mathbf{F}_{\rm W} + \mathbf{F}_{\rm C} + \mathbf{F}_{\rm SS}) + \frac{\mathbf{dv}_{\rm si}}{dt} & \text{if } A \ge 90\% \\ & \text{and } P \ge P_s, \\ \frac{1}{2}(\rho_{\rm si} c_{\rm si} A_{\rm si})|\mathbf{v}_{\rm si} - \mathbf{u}|(\mathbf{v}_{\rm si} - \mathbf{u}) & \text{otherwise.} \end{cases} \quad (2)$$

Iceberg stability criterion, bottom friction and melting parameterizations are included.

Forcing

- Model inputs averaged daily to limit memory storage.
- **Atmospheric forcing** from **ERA-40** reanalysis of the European Center for Medium range Weather Forecasting (ECMWF, *Uppsala et al., 2005*).
- **Ocean variables** supplied by a nested configuration of a **HYbrid Coordinate Ocean Model** (HYCOM, *Bleck 2002*):
  - The sea ice module :
    Dynamic Elastic-Viscous-Plastic rheology sea ice model, (*Hunke et al., 1997*).
    Thermodynamic ice model, (*Drange and Simonsen, 1996*).
  - The inner model covers the Barents and the Kara Seas with an horizontal resolution of 5 km and uses 22 vertical hybrid layers.
  - The outer model is a version of the TOPAZ3 (**http://topaz.nersc.no/**), forecasting system that covers the Atlantic and the Arctic Ocean, run without data assimilation (*Bertino and Lisæter, 2008*).

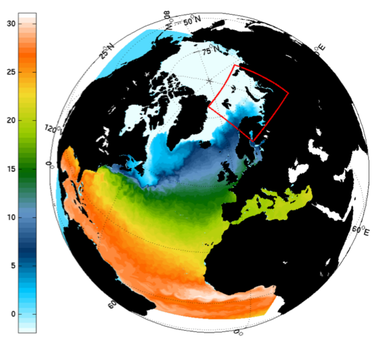

Figure 1: Topaz model SST and limits of the nested model, week 2 of May 1990.

EXPERIMENT

- The iceberg release occurs from July **1985** to December **2005**. The first 1.5 year is the spin-up time.
- The initial iceberg length, width and heigh are generated from a log-normal distribution based on IDAP observations from 1988 to 1990.
- The main iceberg production sites are given on Figure 2.
- The annual iceberg production rate is estimated from *Dowdeswell et al. (2008)* and *Kubyshkin et al. (2006)*.
- The icebergs release is considered as an event occurring at random with a known average rate (annual rate) and independently of the time since the last release (Poisson distribution).

CLIMATOLOGY

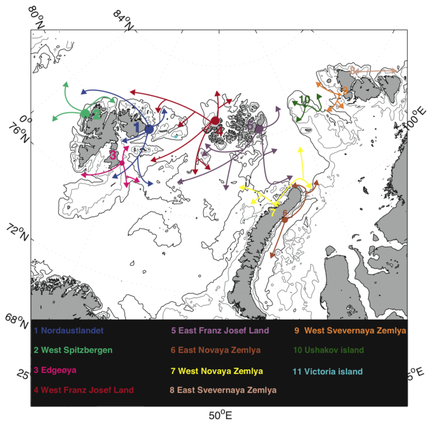

Figure 2: Sketch of the model runs typical pathways of icebergs from their calving site.

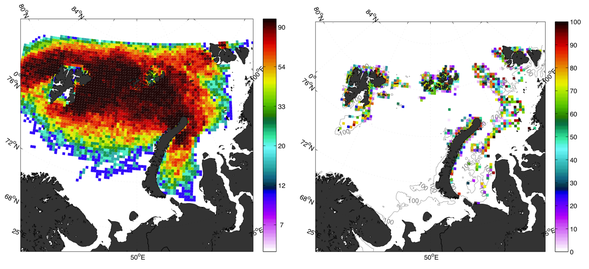

Figure 3: Probability of encountering an iceberg within a year in the domain from 1987 to 2005 on 25 km×25 km grid cell. The scale is logarithmic.

Figure 4: Probability to have an iceberg grounded within a 25 km×25 km grid during the period 1987-2005. Gray contours are isobaths at 100 m.

INTERANNUAL VARIABILITY

Dynamics and thermodynamics

Table 1. Correlations between the annual iceberg extension and the annual sea ice area (SI area), the sea ice volume (SI vol), sea ice transport into the domain, from Svalbard to Severnaya Zemlya (SI trp), the positive transport along Norway-Svalbard section (N-S trp +), the sea surface temperature (SST), for the period 1987-2005.

	SI area	SI vol	SI trp	N-S trp+	SST
			No time lag		
With trend	00.68*	00.13*	00.44**	-0.30n.s	-0.51*
Without trend	00.64*	00.03*	00.41**	-0.28n.s	-0.49*
			One year time lag		
With trend				-0.65*	
Without trend				-0.66*	

* $p \le 0.1$, with a t-test that takes into account the autocorrelation of the iceberg extent, $p \le 0.05$ with a t-test neglecting the autocorrelation of the iceberg extent.
** Same as * with $p \le 0.2$ and $p \le 0.1$ respectively.
n.s The correlation is not significant.

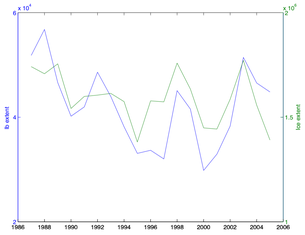

Figure 5: Annual mean of the iceberg extent (blue) and ice extent (green) over the model domain, given in km^2.

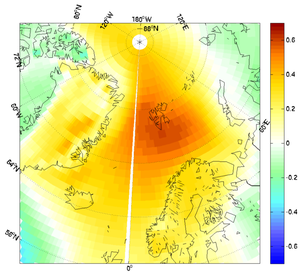

Figure 6: Linear correlation between the annual MSLP anomalies and the iceberg extent **lagged by one year** for the period of study.

The interannual iceberg and sea ice extent are strongly correlated (Table 1). As for the sea ice extent (*Sorteberg and Kvingedal, 2006*), iceberg extent is controlled dynamically by the presence of northerly winds. Both have a weak decreasing trend (Figure 5). Higher than normal MSLP north east of the Greenland and south of Svalbard limits the inflow of warm Atlantic water. It reduces the heat content of the Barents Sea the following year, increasing the mean age of icebergs and thus their potential extension that year (Table 1 and Figure 6).

Extreme southernmost extension

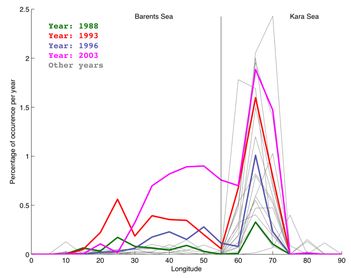

Figure 7: Annual percentage of occurrence found south of 75°N depending on their longitude location for the period 1987-2005. The number was split by classes of 5° of longitude. The colored lines correspond to the years with the largest number of occurrence south of 75°N within the Barents Sea area.

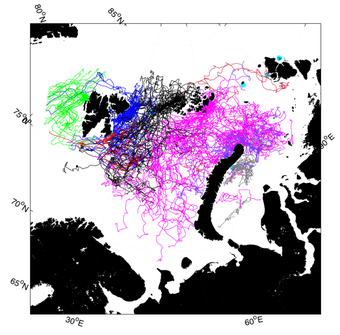

Figure 8: Modeled iceberg trajectories for the year 2003. The colors indicate the different origin sites.

The model captures the anomalous southernmost extension of icebergs that have been observed during expeditions campaigns south east of the Barents Sea in May 2003 (*Zubakin et al., 2004*). The model suggests that they all come from the eastern part of Franz Josef Land archipelago (Figure 8).

REFERENCES

Keghouche, I., L. Bertino, and K. Lisæter, Parameterization of an iceberg drift model in the Barents Sea, *Journal of Atmospheric and Oceanic Technology, 26*(10), 2216–2227.

Keghouche, I., F. Counillon, and L. Bertino, Modeling dynamics and thermodynamics of icebergs in the Barents Sea from 1987 to 2005, *submitted*.

Lichey, C, H. H. Hellmer, Modelling giant-iceberg drift under the influence of sea ice in the Weddell Sea, Antartica, *J. Glaciology, Vol. 47, No. 158*, 2001.

Acknowledgements: The authors acknowledge Trond Mohn c/o Frank Mohn AS for an endowment to the Mohn-Sverdrup Center. This work has also received a grant for computer time from the Norwegian Program for supercomputing (NOTUR).